



Research paper

Development of a pilot-scale manufacturing process for protein-coated microcrystals (PCMC): Mixing and precipitation – Part I

Corinna König^a, Karoline Bechtold-Peters^{a,*}, Verena Baum^a, Torsten Schultz-Fademrecht^a, Stefan Bassarab^a, Klaus-Jürgen Steffens^b^a Boehringer Ingelheim Pharma GmbH & Co. KG, Biberach an der Riss, Germany^b Department of Pharmaceutical Technology, University of Bonn, Bonn, Germany

ARTICLE INFO

Article history:

Received 2 September 2010

Accepted in revised form 17 November 2011

Available online 26 November 2011

Keywords:

Precipitation

Protein

Microcrystals

PCMC

Stabilisation

Impingement jet mixer

ABSTRACT

A novel protein-coated microcrystal (PCMC) technology offers the possibility to produce dry protein formulations suitable for inhalation or, after reconstitution, for injection. Micron-sized particles are hereby produced by co-precipitation via a rapid dehydration method. Thus, therapeutic proteins can be stabilised and immobilised on crystalline carrier surfaces. In this study, the development of a continuous manufacturing process is described, which can produce grams to kilograms of PCMC. The process chain comprises three steps: mixing/precipitation, solvent reduction (concentration) and final drying. The process is published in two parts. This part describes the mixing and precipitation performed using continuous impingement jet mixers. Mixing efficiency was improved by dividing the anti-solvent flow into two or four jets, which were combined again inside the mixer to achieve an embracing of the aqueous solution (sandwich effect). The jets provided high energy dissipation rates. The anti-solvent jets (95% of the total volume) efficiently mixed the protein-carrier containing aqueous solution (5% of the total volume), which was demonstrated with computational fluid dynamics and the Villermaux–Dushman reaction. The improved mixing performance of the double jet impingement (DJI) or the quadruple jet impingement (QJI) mixers showed a positive effect on easily crystallising carriers (e.g. DL-valine) at laminar flow rates. The mixer and outlet tube bore size was 2.0–3.2 mm, because smaller sizes showed a high tendency to block the mixer. The mixing effect by impaction was sufficiently high in the flow rate range of 250–2000 mL/min, which corresponds to the transition from laminar to turbulent flow characteristics. At lower flow rates, mixing was enhanced by ultrasound. 50–80 L PCMC suspension was readily produced with the QJI mixer.

© 2011 Elsevier B.V. All rights reserved.

1. Introduction

Biological molecules have become an important category of therapeutic drugs for the treatment of life-threatening and chronic diseases in the past few decades [1,2]. Due to poor oral bioavailability, most biopharmaceuticals are delivered by injection. During the development of liquid protein formulations, stabilisation is crucial, because proteins can undergo a variety of chemical and physical degradation reactions. If an aqueous liquid formulation is not sufficiently stable, long-term stability can be improved by conversion into dry protein formulations [3–5]. Therefore, commercially available protein drugs are often lyophilised products [4]. However, process-related protein degradation can still occur

during the freezing and drying phases, e.g. due to cryo-concentration phenomena [5].

Especially for alternative routes of drug delivery such as the pulmonary or nasal route, or for admixture into a depot formulation or filling of an implantable device, alternative drying techniques have been explored, which produce micron-sized and dispersible powders as opposed to protein cakes. These include spray drying [6], precipitation followed by vacuum drying [7], spray-freeze drying [8,9], supercritical fluid drying [10–12] and crystallisation/precipitation methods [13,14].

Particularly with regard to cost-effectiveness, precipitation methods are attractive. An interesting method is the protein-coated microcrystals (PCMC) technology that stabilises biomolecules on crystalline surfaces by co-precipitation during rapid solvent exchange [15]. To prepare these microcrystals, the protein is dissolved in a concentrated aqueous solution of crystal-forming carriers, e.g. amino acids and/or salts. This aqueous solution is rapidly and thoroughly mixed with a water-miscible organic solvent, resulting in the formation of the PCMC. The precipitated particles are typically

* Corresponding author. Boehringer Ingelheim Pharma GmbH & Co. KG, Birkenfelder Straße 65, 88397 Biberach an der Riss, Germany. Tel.: +49 7351 54 94910; fax: +49 7351 54 94890.

E-mail address: karoline.bechtold-peters@gmx.net (K. Bechtold-Peters).

micron-sized. These particles in suspension can be concentrated and dried to form a free-flowing powder. Protein-coated microparticles can be injected after reconstitution or used for alternative routes of drug delivery. The chemical and physical stability of biomolecules was investigated in various studies [16–19].

The focus of the work reported in this paper was to develop a continuous pilot-scale process to produce grams to kilograms of PCMC powder, appropriate for GMP purposes that would also be adaptable for use under aseptic conditions. Previously, only small amounts of PCMC have been produced in a batch mode using pipettes and lab-scale equipment.

The continuous process comprises three steps, as shown in Fig. 1a. The first step is the mixing and precipitation of the PCMC, the second step the optional solvent reduction (concentration) and the third step the final drying to harvest a dry stabilised protein powder. Development of the process, using appropriate model proteins, is published in two research papers (Part I and II).

This paper presents the work performed to develop the first step. The influence of flow rates and of ultrasound as mixing aids was investigated in depth. A homogeneous precipitation can only be achieved if a surplus of water-miscible organic solvent is rapidly and efficiently mixed with the aqueous solution containing protein, carrier and further ingredients. Therefore, the specific challenge was the unfavourable mixing ratio of 95:5. In order to see the maximum impact of process conditions and type of mixing equipment, a sensitive model protein, trypsin, and suboptimal formulations were chosen.

2. Materials and methods

2.1. Materials

2.1.1. Production of trypsin PCMC

100 g Glycine (Tessenderlo Chemie S.A., Belgium) was dissolved in 1 L of a solution containing 10 mM CaCl_2 -hexahydrate (Merck, Germany), 10 mM NaCl (Südsalz, Germany) and purified water. 11.4 g lyophilised trypsin powder served as a sensitive model protein (T 0303, Sigma–Aldrich, Germany) and was added to the glycine solution.

Alternatively, 40 g of DL-valine (Fluka, Germany) was dissolved in 1 L of a solution of 5 mM CaCl_2 -hexahydrate and 5 mM NaCl in purified water. Subsequently, 4.6 g of lyophilised trypsin powder was dissolved in the DL-valine solution, to give in both cases target protein loadings of about 9%. Protein loading is defined as the

amount of protein in % (w/w) related to the total dry mass of the resulting powder.

Each solution was filtered over a Durapore™ membrane (0.45 μm , Millipore, USA). Five parts of the protein-carrier solution were immediately mixed with 95 parts of the anti-solvent isopropyl alcohol (Aug. Hedinger GmbH & Co. KG, Germany).

2.2. PCMC containing mAb I and mAbII

Monoclonal antibodies (mAbI, mAbII) were kindly provided by Boehringer Ingelheim (Biberach, Germany). MAb I was dispersed in a solution that contained glycine and various salts. The resulting protein-carrier solutions contained 80 g/L glycine, 13.4 g/L buffer salts and 6.1 g/L mAbI. 15.9 g/L mAb II was dissolved in a solution of 137 g/L glycine and 9.8 g/L buffer salts. The protein-carrier solutions were filtered particle-free. Five parts of the protein-carrier solution were mixed immediately with 95 parts of the anti-solvent. The anti-solvent of mAb I and mAb II was 2-methylpropane-1-ol (270,466, Sigma–Aldrich, Germany).

2.3. Mixing process methods

The protein-carrier solution (5% of the final volume) was mixed with an excess of anti-solvent (95% of the final volume) with different continuous flow mixers. For precipitation, T-, Y- and X-mixers (Kartell, Italy) are often used. In this work, the focus was placed on the X-mixers, namely a double jet impingement (DJI) mixer, due to its ability to provide rapid mixing. Impinging jets can produce energy dissipation rates of up to 10^5 W/kg compared to single turbulent jets with $\sim 10^4$ W/kg, rotor stator mixers with $\sim 10^2$ W/kg and stirred tanks, centrifugal pumps or turbulent pipes with ~ 0.1 – 10 W/kg [20,22].

In the first set of experiments, mixing with an X-mixer with an inner diameter of 2.0–3.2 mm was enhanced by an ultrasonic bath (35 kHz, 150–300 W, Brandelin Sonorex Digital 10 P) at a total flow rate of 150 mL/min, while the X-mixer and the outlet tube were placed inside the bath.

Next, an Ultrasonic Vortex Crystalliser (UVC, Prosonix, UK) was tested for mixing and precipitation, again at a total flow rate of 150 mL/min. The UVC uses vortex-flow dynamics to promote efficient mixing of two or three liquid streams with or without the help of ultrasound (40 kHz, 8 W). The UVC has three tangential inlets as well as an axial outlet, and on the opposite wall, an ultrasound probe is mounted. The probe delivers the ultrasound

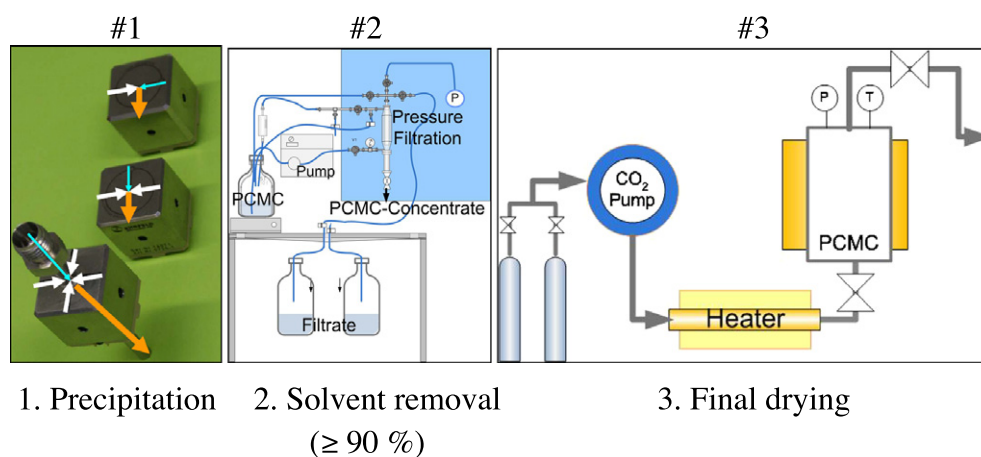


Fig. 1a. Process chain to produce protein-coated microcrystals: #1. Mixing/precipitation step, where PCMCs are co-precipitated from an aqueous mixture containing a saturated solution of carrier, precipitation-protective or -stabilising additives and protein with an excess of water-miscible solvent using static impingement jet mixers, #2. Solvent removal step by modified pressure filtration (MPF), #3. Final drying step by extraction with supercritical CO_2 (SFE).

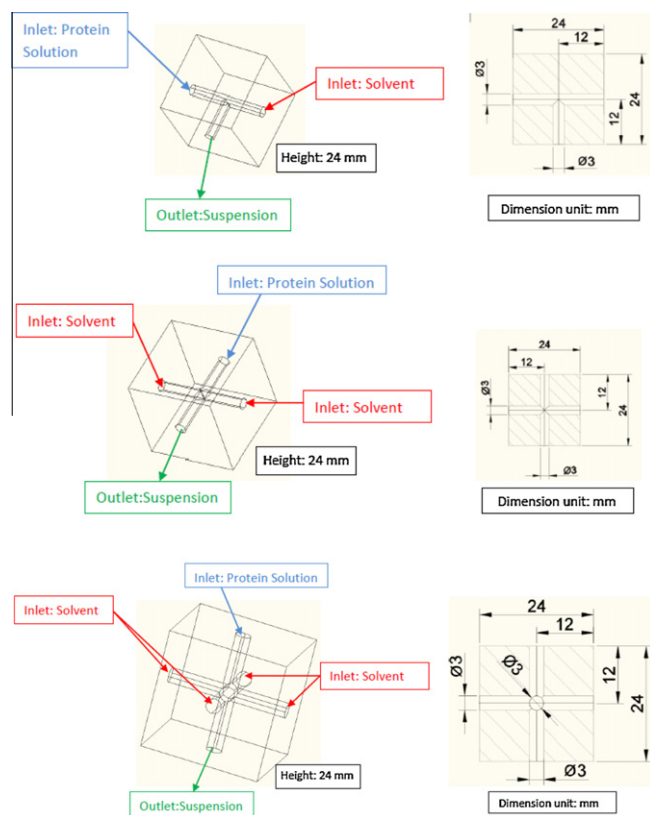


Fig. 1b. Static impingement jet mixers – top: single jet impingement mixer (SJI), centre: double jet impingement mixer (DJI), bottom: quadruple jet impingement mixer (QJI) 20 μ m.

impulse directly into the middle of the vortex mixing chamber. The vortex mixing chamber is cylindrical with a diameter of 20 mm and contains no baffles to disrupt the vortex flow.

The second set of experiments concentrated especially on the X-mixer (Kartell, Italy) with an inner diameter of 3.2 mm at total flow rates of 250–1000 mL/min, but without any additional ultrasonification. The mixer enabled a separation of the anti-solvent streams into two streams, which were combined again inside the mixer.

In the third set of experiments, the T-mixer (single jet impingement SJI), the X-mixer (DJI) and the QJI mixer were compared. All three mixers were mass transfer mixers with a bore size of 3 mm. The three mixers were constructed at Boehringer Ingelheim in the company's workshops using stainless steel modules from Ehrfeld Mikrotechnik BTS (Germany). The difference between the mixers was the number of anti-solvent inlets. The SJI had only one, the DJI two and the QJI four inlets for the organic solvent (Fig. 1b). The impact of the constructional differences were simulated by computational fluid dynamics (CFD) using the program Fluent (ANSYS, USA).

The resulting suspensions had a solids content of 0.23–0.57% (w/v) and were separated into solid and liquid phase by membrane filtration (Durapore™, 0.45 μ m, Millipore, USA). The harvested filtration cakes, which were still wet, were air-dried inside a box flushed by dry air.

2.4. Analytical methods

2.4.1. Size Exclusion Chromatography (HP-SEC)

A TSK2000SWXL 300 \times 7.8 mm column (Tosoh Biosep, USA) was used to determine the monomer content. 40 mg of PCMC corresponding to ~3.6 mg of trypsin was dissolved in 1 mL Tris-buffer

(4.6 mM trometamol-HCl, 11.5 mM CaCl₂·6H₂O) and filtered particle free (0.45 μ m PVDF syringe filter, Roth). The mobile phase was prepared by dissolving 70.13 g NaCl, 15.60 g NaH₂PO₄·H₂O in 2 L water, adjusted to a pH of 7.0, and was passed through a 0.2 μ m filter prior to use. The mobile phase was delivered to the column at a flow rate of 1.0 mL/min using the ÄKTA-explorer (GE-Healthcare Life Science, UK) equipped with an auto sampler. Chromatograms were recorded with an absorbance detector at λ = 280 nm. Trypsin standards with a concentration range of 2.0–10.0 mg/mL were prepared from unprocessed material. The injection volume was 25 μ L. Monomer, aggregate and fragment contents were expressed as a percentage of the total area under the curve (AUC) using the Unicorn software. In this work, the monomer content was calculated relative to the content of unprocessed trypsin.

2.4.2. UV/VIS spectroscopy

After reconstitution of the PCMC, the protein absorption was measured at 280 nm using a λ UV/VIS spectrophotometer (Perkin-Elmer, Germany). Absorption at 320 nm was subtracted from the value measured at 280 nm. The calibration curve showed a R^2 = 0.9998 after linear regression analysis. The measured trypsin concentration was compared to the theoretical trypsin concentration and the percentage protein recovery (PR) calculated.

2.4.3. Assessment of protein binding by centrifugation and UV/VIS spectroscopy

With this analytical model, only PCMC with strong non-covalent interaction between protein and carrier can be recovered, and hence measured by UV/VIS spectroscopy after centrifugation and reconstitution of the resulting pellet. PCMC with weakly bound protein lose to various degrees the superficial protein due to shear stress during centrifugation.

50 mL of PCMC suspension was centrifuged at 1000 g for about 15 min (Biofuge primo, Heraeus, Germany). The supernatant was removed and the pellet redispersed in 30 mL anti-solvent. The crystals of the dispersion were harvested by membrane filtration (Durapore, 0.45 μ m, Millipore, USA) and air-dried. The protein attached to the redissolved crystals were analysed by UV/VIS spectroscopy, as described above.

2.4.4. Laser diffraction (LD)

The PCMC particle sizes in suspension were determined by laser diffraction with the Sympatec Helos system using a 50-mL cuvette (Sympatec GmbH, Germany). The suspension was stirred at 500 rpm, dispersed with an air pressure of 3 bar and passed through a parallel laser beam in front of the Fourier lens (50 or 100 mm). The particle size distribution was calculated using the Fraunhofer model and expressed as volume distribution (Q_3). The median x_{50} and the span 90 $(x_{90} - x_{10})/x_{50}$ were used to compare the sizes of PCMC production.

2.4.5. Scanning electron microscopy (SEM)

SEM images (Supra 55 VP, Carl Zeiss SMT AG, Germany) were used to examine the morphology of the dried particles. Double-sided tape fixed the particles, and the conductivity was enhanced by a thin layer of gold/palladium.

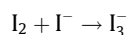
2.4.6. X-ray powder diffraction (XRPD)

Crystallinity and polymorphic form of the carrier in PCMC were assessed using a STOE Stadi P X-ray diffractometer with position-sensitive detector and stationary copper anode (40 kV, 40 mA). X-ray diffraction diagrams were recorded between 3° 2 θ and 40° 2 θ .

2.4.7. Villiermaux–Dushman reaction

The parallel reaction was employed to verify the computational fluid dynamics calculations. The reaction is based on two solutions: The first solution contains 0.1 mol/L H₂SO₄ and the second solution 0.5 mol/L H₃BO₃, 0.25 mol/L NaOH, 0.007 mol/L KIO₃ and 0.035 mol/L KI. The solutions were mixed at a ratio of 5 parts of the first solution to 95 parts of the second solution. Inside the mixers (SJI, DJI, QJI), the following reactions take place:

1. $\text{H}_2\text{BO}_3^- + \text{H}^+ \rightarrow \text{H}_3\text{BO}_3$ (fast reaction)
2. $\text{IO}_3^- + 5\text{I}^- + 6\text{H}^+ \rightarrow 3\text{I}_2 + 3\text{H}_2\text{O}$ (slow reaction)



Reaction 1 is very fast and captures the H⁺. If mixing is efficient, only few H⁺ ions are available for reaction 2. Consequently, the accumulated amount of I₃[−] ions is low. The I₃[−] ions are indicative of the mixing efficiency and can be measured by UV ($\lambda = 353 \text{ nm}$).

2.4.8. Turbidity

The precipitation kinetics can be detected by outline turbidity measurement (Hach 2100 AN, Hach-Lange, Germany). Depending on mixer and process conditions, the compounds of the mixed solutions precipitate more slowly or more rapidly. An aliquot of the collected suspension was investigated until a turbidity value of 120 FNU (Formazin Nephelometric Units) was reached as the endpoint. The time was noted.

3. Results and discussion

3.1. Mixing/precipitation step

The basic requirement is fast and homogenous mixing to permit uniform precipitation of the protein-coated microcrystals (PCMC).

At the beginning, micron-bore (<1 μm) DJI mixers were used. With a bore size below 1 μm and a flow rate of 5–15 mL/min, the mixer and the outlet capillary often became blocked and could not be flushed free by the action of the pumps. This would lead to long production times and would not meet the target to develop a pilot-scale process capable to generate at least 500 g of PCMC (dry mass) or the corresponding suspension in a single shift (of 8 h). Consequently, the mixer and outlet tube diameters were enlarged to 2 mm or even 3 mm. Earlier screening experiments described a significant effect of the bore diameter on the quality of the PCMC. By enlarging the bore diameter, the size of the microparticles increased and protein recovery in the dry PCMC decreased. This was attributed to the inappropriate and too-slow mixing of the

two solutions. In order to improve mixing efficiency, two strategies were pursued.

The first strategy was to support mixing and precipitation by application of ultrasound. The second strategy was to increase the flow rate to shift the flow characteristics in the mixer towards the turbulent range. Ultrasound produces cavitations at the used frequency of 35–40 kHz. The implosion of the cavitations accelerates the diffusion process and promotes a rapid mixing in a small space within a short time. Moreover, sonocrystallisation can be used to initiate nucleation, i.e. it decreases the induction time for nucleation and improves primary and secondary nucleation [21]. The DJI mixer and the outlet tube ($\varnothing = 2.0 \text{ mm}$) were placed in a full-powered ultrasound bath, which generated an indirect ultrasound impulse on the mixing. The flow rate was 150 mL/min. The mixing was clearly improved by the use of the ultrasound that resulted in an increased protein recovery of 67% instead of 22% without ultrasound (Table 1). Furthermore, smaller particles with a median diameter of 6.5 μm compared to 20.8 μm without ultrasound were recorded. These significantly smaller particles resulted from the improved mixing brought about by the ultrasound, which supported formation of crystal nuclei rather than crystal growth. The crystals may have been shattered by collision in microjet streams induced by ultrasound, since a very broad particle distribution (span 90 = 5.8) resulted. Without ultrasound, the span 90 was around 2. In a further experiment, the impact of the ultrasound bath was assessed for a DJI at a bore size of 3.2 mm and a flow rate of 250 mL/min. Here, nearly the same particle size of 20 μm and a protein recovery about 100% were seen, irrespective of the use of ultrasound. However, a slightly higher loss of monomers (monomer content 75%) and a narrower particle size distribution with a span of 1.3 were measured with the ultrasound-assisted sample (Table 1). In this experiment, the diffusion process was not further improved by the indirect ultrasound impulse as a consequence of shorter ultrasound contact time at higher flow rates. Moreover, there seems to be a slightly negative impact on protein integrity by ultrasound as assessed by the monomer content (75% vs. 78%), although the results may have been compromised by the autocatalytic activity of the model protein trypsin.

Another set of experiments evaluated a direct ultrasound impulse inside the mixing chamber. An Ultrasonic Vortex Crystalliser (UVC) was used to produce PCMC. The flow rate was 150 mL/min. Co-crystals precipitated under ultrasound had a median particle size (x_{50}) of 20 μm and were somewhat smaller than the PCMC produced without ultrasound. The particle size distribution was nearly the same, and the protein recovery was 100% for all samples. Even the monomer content showed no difference between samples, but was low (~65%). Evidently, the mixer itself already had a negative impact on protein integrity independently of

Table 1

Mixing/precipitation conditions and results on the PCMC quality were evaluated by monomer content, particle size in suspension (x_{50} and span 90) and protein recovery (PR) of the model protein trypsin coated onto glycine.

Mixer	ID of outlet tube (mm)	Total flow rate (mL/min)	Process conditions (Re)	Relative monomer content (%)	Particle size		
					x_{50} (μm)	Span 90	PR (%)
First strategy: precipitation with the help of ultrasound							
DJI	2.0	150	With ultrasound	No value	6.5 ± 1.0	5.8	67 ± 6.5
DJI	2.0	150	Without ultrasound	No value	20.8 ± 0.1	2.1	22 ± 1.2
DJI	3.2	250	With ultrasound	75.0 ± 0.1	20.5 ± 0.2	1.3	103 ± 1.1
DJI	3.2	250	Without ultrasound	78.0 ± 0.1	18.9 ± 0.1	2.5	105 ± 1.1
UVC	20	150	With ultrasound	65.4 ± 2.6	20.2 ± 0.3	1.9	100 ± 0.1
UVC	20	150	Without ultrasound	64.8 ± 0.5	24.6 ± 0.2	2.0	100 ± 1.8
Second strategy: precipitation by increasing flow rate							
DJI	3.2	250	Laminar (589)	78.0 ± 0.1	18.9 ± 0.1	2.5	105 ± 1.1
DJI	3.2	500	Laminar (1190)	82.0 ± 0.1	17.1 ± 0.1	2.0	104 ± 1.0
DJI	3.2	1000	Turbulent (2380)	80.0 ± 0.1	12.4 ± 0.1	2.0	106 ± 1.0

SJI = single jet impinger; DJI = double jet impinger; QJI = quadruple jet impinger; UVC = ultrasonic vortex crystalliser.

the use of ultrasound. In all experiments with ultrasound, no blockage of the mixer or the outlet tube was observed by precipitates, which clearly constitutes a big advantage.

Comparing the DJI mixer and the UVC, a significant impact of the mixer type on the protein quality was found. In the hydrodynamic UVC, trypsin was more degraded than the in DJI. The monomer content was about 10% lower with the UVC (Table 1) compared to the DJI, the latter was found to exert obviously less stress on the model protein. With the DJI, the mixing conditions were laminar (Reynolds number <2300) resulting in lower shear forces during mixing and precipitation. These findings supported the second strategy to enhance the mixing and precipitation by increasing the total flow rate.

In the next set of experiments, the DJI mixer was run at total flow rates between 250 mL/min and 1000 mL/min. A steady flow rate is very important for a constant mixing ratio. Typical flexible-tube peristaltic pumps revealed changes in flow rate when the pressure rose due to crystals sticking to the mixing system. For that reason, micro annular gear pumps were introduced (Hydraulik Nord Parchim Mikrosysteme, Germany). The impact of increasing flow rates is summarised in Table 1. Indeed, with increasing flow rates, the particle size of the PCMC decreased from 19 µm to 12 µm. All protein was recovered on the crystal surfaces. The relative monomer content ranging from 78% to 82% showed no differences. The monomer content of the model protein trypsin decreases during analytics if the samples are not measured immediately because of autocatalysis (monomer content drop of 3% over 21 h). At turbulent flow, the resulting particle morphology was more homogeneous compared to the samples produced at laminar flow, as seen in Fig. 2. PCMC can be produced with the DJI at laminar and turbulent flow, but the turbulent flow improves the uniformity of the product.

3.2. Comparison of impingement mixers

The impingement mixers differ in the number of tangential inlets for the anti-solvent (Fig. 1a). The SJI has only one, the DJI two and the

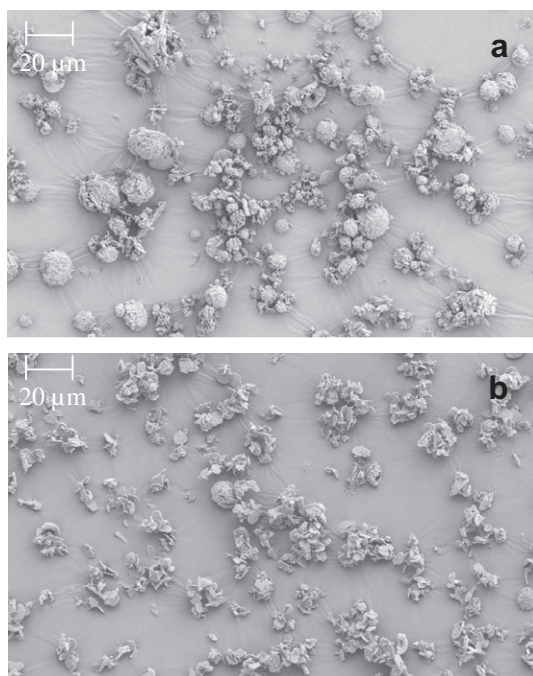


Fig. 2. SEM of trypsin-glycine microcrystals produced with the DJI mixer at flow rates of: (a) 250 mL/min and (b) 1000 mL/min.

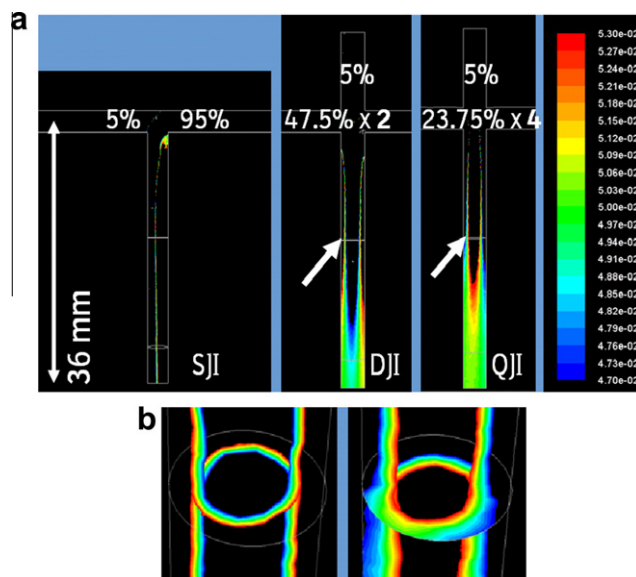


Fig. 3. Pictures of computational fluid dynamic simulations at 750 mL/min flow (a) three mass transfer mixers (SJI, DJI, QJI). (a) The colour green indicates perfect mixing, the colour red means there is still too much water, the colour blue indicates too much anti-solvent and the colour black stands for a water content below 4.7% or higher than 5.3%, (b) Enlarged and canted profile of the arrow – left DJI, right QJI.

innovative QJI mixer has four anti-solvent inlets. The protein-carrier solution is always fed into the mixer through one inlet.

The pictures of computational fluid dynamic simulations (Fig. 3) illustrate the differences in mixing efficiency. With the SJI, at a mixing distance of 36 mm, diffusion between the two solutions was not finished compared to the DJI and QJI. Especially, the QJI produced a homogeneous mixture (symbolised by the green colour) at a mixing distance of 36 mm. A uniform green colour means optimal mixing and achievement of the target water content of 5%. For the DJI, the black zone (water content <4.7% or >5.3%) at 36 mm mixing distance is larger compared to the QJI.

The fluid dynamic simulations also revealed basic differences between DJI and QJI in the mode of mixing. For the DJI, the protein-carrier solution flows into the middle of the mixer and the two flows of the preponderate anti-solvent press the protein-carrier solution onto the walls of the mixer outlet, as the red colour

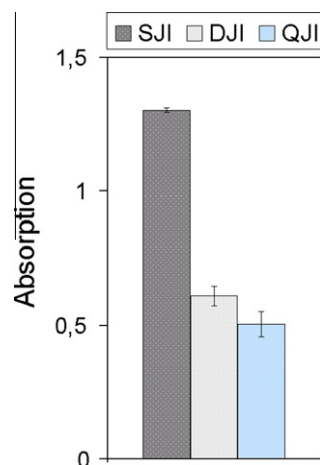


Fig. 4. Mixing comparison of the SJI, DJI, QJI mixer by using the Villiermaux-Dushman reaction at a flow rate of 750 mL/min – average, standard deviation of six single experiments. (For interpretation of the references to colour in this figure legend, the reader is referred to the web version of this article.)

illustrates in Fig. 3b. In contrast, for the QJI, the axially introduced protein-carrier solution is caught by the four tangentially running anti-solvent flows in the middle of the mixer, like a sandwich. Therefore, this effect is called the sandwich effect. The red colour in Fig. 3b symbolises the border to the protein-carrier solution.

The simulation showed that mixing and diffusion efficiency increase in the series $SJI < DJI < QJI$. This was verified by a chemical reaction from Villiermaux–Dushman. An acid solution (5% of the total volume) was mixed with an iodate, iodide and borate ions containing solution (95% of the total volume). Upon rapid mixing and diffusion, only the fast reaction of the borate ions with the protons proceeds. Otherwise, the iodate and iodide ions undergo a slow reaction to iodine. The iodine reacts with iodide ions to tri-iodide, which was measured with an UV/VIS spectrophotometer at a wavelength of 353 nm. High UV absorption means poor mixing. Fig. 4 depicts the average and the standard deviation of six independent measurements. The QJI showed the best mixing with an absorption of 0.5. The mixing efficiency of the DJI was slightly worse with an absorption value of 0.6. The absorption of the SJI was 1.3, the worst mixing performance of these three mass transfer mixers. In summary, the results of the Villiermaux–Dushman reaction confirmed the simulation results. The mixing efficiency improved in the order $SJI < DJI < QJI$.

Finally, the three mixers were tested for their performance in PCMC precipitation. With the three mass transfer mixers, trypsin-glycine co-crystals were produced at a turbulent total flow rate of 1000 mL/min. The results are summarised in Table 2. All three mixers produced the same PCMC quality. Owing to the fast crystallisation kinetics of the carrier glycine, it seems that perfect mixing is not really necessary. Neither at laminar flow rates (500 mL/min, data not shown) nor at turbulent flow rates (1000–2000 mL/min) were significant differences seen. Therefore, the system was challenged by DL-valine, a slower crystallising carrier. The model protein was again trypsin, and the loading rate was 10%. Mixing/precipitation was performed at laminar flow of 500 mL/min up to turbulent flow of 2000 mL/min. The time was recorded until a turbidity of 120 FNU was reached (=TT 120) as an indicator of the precipitation of the trypsin-loaded DL-valine crystals. Nuclei formation was faster at turbulent flows (1000–2000 mL/min) compared to the laminar flow (500 mL/min), as can be seen in Fig. 5. Whereas at laminar flows, the TT 120 was longest for the SJI, the differences between the mixers were eliminated at turbulent flows. The particle size analyses partly reflected the results of the turbidity measurements. At laminar flow, the particle size was 34–44 μm , thus larger compared to the samples produced at the turbulent flows (10–34 μm in Fig. 6a). The impact of the flow rate on particle size was dependent on the mixer used. Especially, the particles produced by the SJI decreased in size with a rising flow rate, which was less pronounced with the DJI or QJI. At low flow rates, the SJI and QJI resulted in comparable particle sizes, whereas in the turbulent range, the SJI gave the smallest PCMC. Presumably, the method of mixing had an impact on how the crystals were formed and grew. In the QJI, the aqueous solution was caught by the four anti-solvent inlets in the middle of the mixers like a sandwich. In contrast, with the DJI, the aqueous solution was pressed onto the walls of the mixer outlet. This collision probably initiated the crystallisation, which was followed by crystal growth on the crystal surfaces.

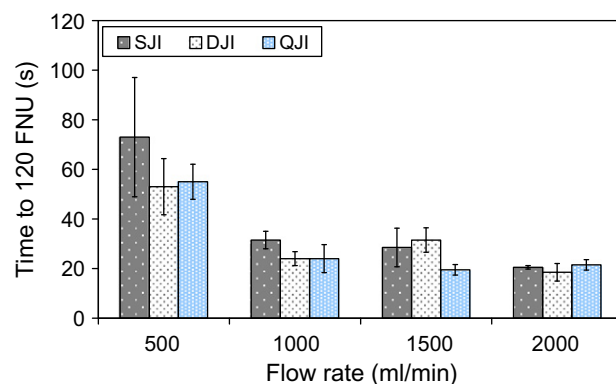


Fig. 5. Time until a turbidity of 120 FNU was reached by three mixers and at various flow rates, trypsin-DL-valine microcrystals.

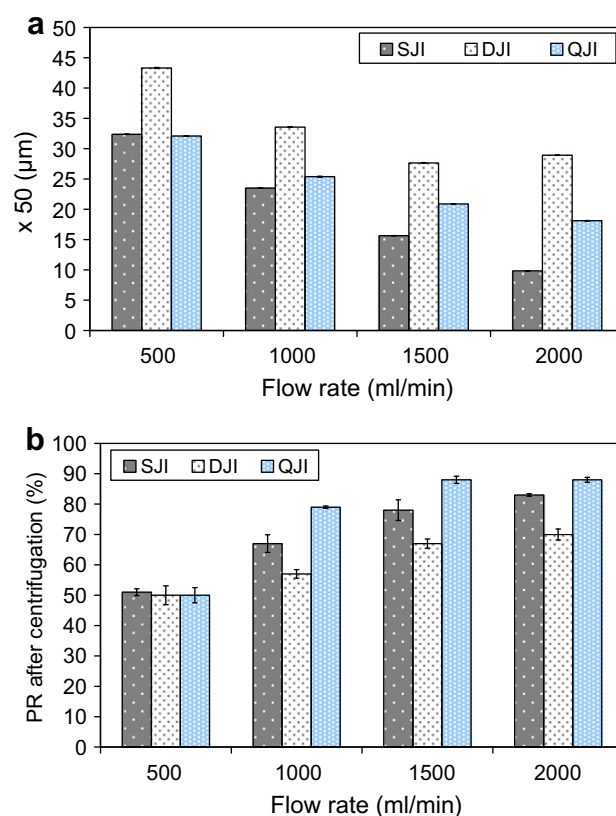


Fig. 6. Characteristics of trypsin-DL-valine microcrystals depending on mixer type and flow rate. (a) Mean particle size of volume distribution (x_{50}). (b) Protein recovery (PR) after centrifugation of the PCMC suspension to evaluate the strength of the non-covalent protein binding on the crystal surface.

Assessing protein recovery after centrifugation of the PCMC suspension and differences between the mixers were seen as well (Fig. 6b). Good protein recovery after centrifugation reflects strong

Table 2

Precipitation of trypsin-glycine microcrystals with different mass transfer mixers (average and standard deviation of several production runs).

Mixer	ID (mm)	Flow rate (mL/min)	Process conditions	x_{50} (μm)	Span 90	PR (%)
<i>Variation of the mass transfer mixer</i>						
SJI	3.0	1000	Turbulent	8.9 ± 0.2	2.0	106 ± 1.0
DJI	3.0	1000	Turbulent	9.9 ± 1.5	2.0	101 ± 1.0
QJI	3.0	1000	Turbulent	8.0 ± 1.4	2.0	100 ± 1.0

non-covalent interactions between carrier and protein. In the laminar range, protein recovery was low (50%) for all samples. It increased dramatically as a consequence of increased flow rates, which suggests good stabilisation. Above 1000 mL/min, the highest protein recovery was always recorded for the QJI, followed by the SJI.

In summary, the computational fluid dynamic simulations and the Villiermaux–Dushman reactions showed a mixing and diffusion improvement in the order SJI < DJI < QJI. The precipitation reactions did not quite follow this ranking, but revealed that the most robust performance as regards TT 120 and particle size over a range of flow rates can be achieved by using the QJI.

3.3. Production of large quantities

The QJI was fixed on a base plate, five inlets and one outlet connected, and was equipped with flow and pressure controllers. Annular gear pumps pressure rated up to 20 bar were used to feed the streams. During the process, occasionally blockages were noticed due to sticking crystals, but these were flushed out by changing the pressure profile (Fig. 7). The pressure showed occasionally pressure peaks up to 18 bar, but dropped again to the normal production pressure of about 1–2 bar. The productions depicted in Fig. 6 were run at laminar flow of 500 mL/min. Up to 80 L of PCMC, suspension was continuously processed, despite the pressure peaks. The target pilot-scale volume of a PCMC suspension of 80 L (for the glycine formulation) corresponding to 500 g PCMC (dry mass) can be produced easily with impingement mixers in less than 3 h, or considering equipment preparation and cleaning time in less than one 8 h shift.

3.4. Protein integrity after precipitation/mixing step and characterisation of carrier crystallinity

Since trypsin might be a useful model to differentiate between manufacturing conditions, we were interested to test the novel technology also for more relevant biological molecules. Two monoclonal antibodies of the IgG type (mAb I and mAb II) were, therefore, selected for further evaluation.

In a first series of experiments, mAb PCMC suspensions (manufactured at 1000 mL/min and 23 °C processing temperature using the DJI) were held for various times at room temperature before filtration, drying and analysis after reconstitution. Both monoclonal antibodies revealed good stability over 2 days if analysed for soluble aggregates (>97% monomers), but behaved very differently if turbidity after reconstitution was considered. An increase in turbidity observed for mAb II indicated formation of larger non-soluble aggregates that escaped HPSEC analysis. mAb I did not show any turbidity changes over 2 days in suspension (Fig. 8). Hence,

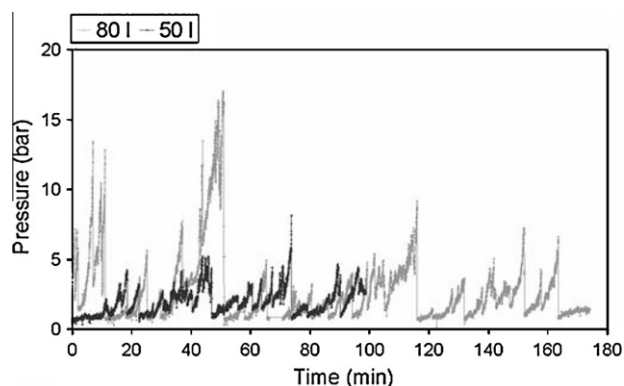


Fig. 7. Pressure profile during a production of 50 L and 80 L of PCMC suspensions (glycine microcrystals) manufactured using the QJI at 500 mL/min.

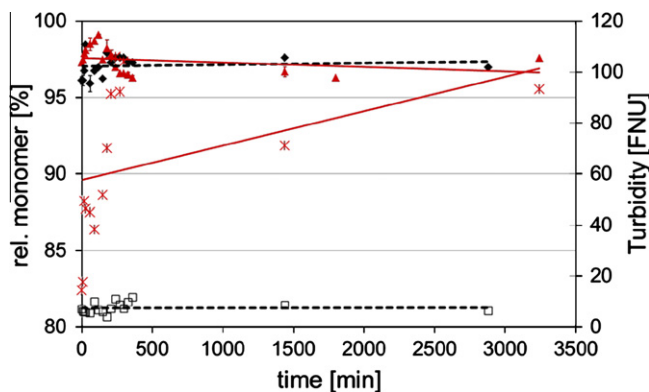


Fig. 8. Protein integrity in mAb PCMC suspensions over holding time at room temperature (◆) relative monomer content and (□) turbidity after reconstitution in suspension of mAb I PCMC, (▲) relative monomer content and (x) turbidity after reconstitution in suspension of mAb II PCMC. (For interpretation of the references to colour in this figure legend, the reader is referred to the web version of this article.)

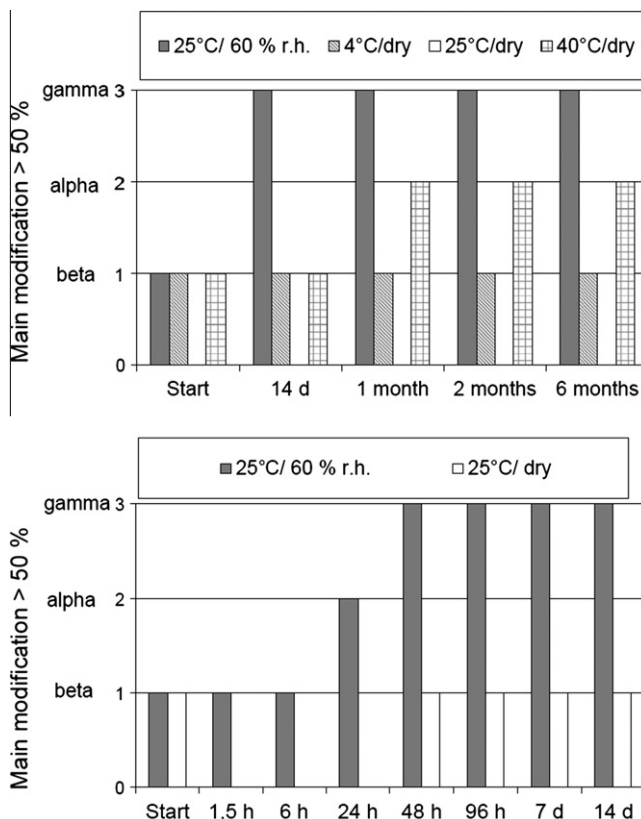


Fig. 9a. Polymorphic modifications of mAb I Glycine PCMC after various storage conditions and storage times (X-ray diffraction data).

dependent on the therapeutic molecule, a processing window of 10 h up to 48 h exists and enables a pharmaceutical process.

The formulations tested involved predominantly water soluble amino acids such as DL valine and glycine. For glycine, three polymorphic modifications are described, and stability of the polymorphs increases at room temperature according to $\beta < \alpha < \gamma$. β -glycine is the metastable form that irreversibly transforms into α - or γ -glycine under moist conditions. Glycine crystallises during PCMC production kinetically controlled as β -modification (Fig. 9a). We were interested to investigate whether the proteins immobilised on the carrier surfaces inhibited polymorphic transformation during storage and to evaluate the consequences of a

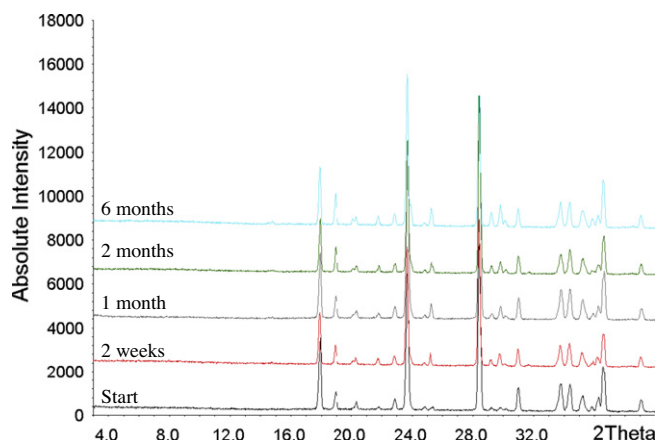


Fig. 9b. X-ray diffraction diagrams of mAb I Glycine PCMC after dry storage at 25 °C. (For interpretation of the references to colour in this figure legend, the reader is referred to the web version of this article.)

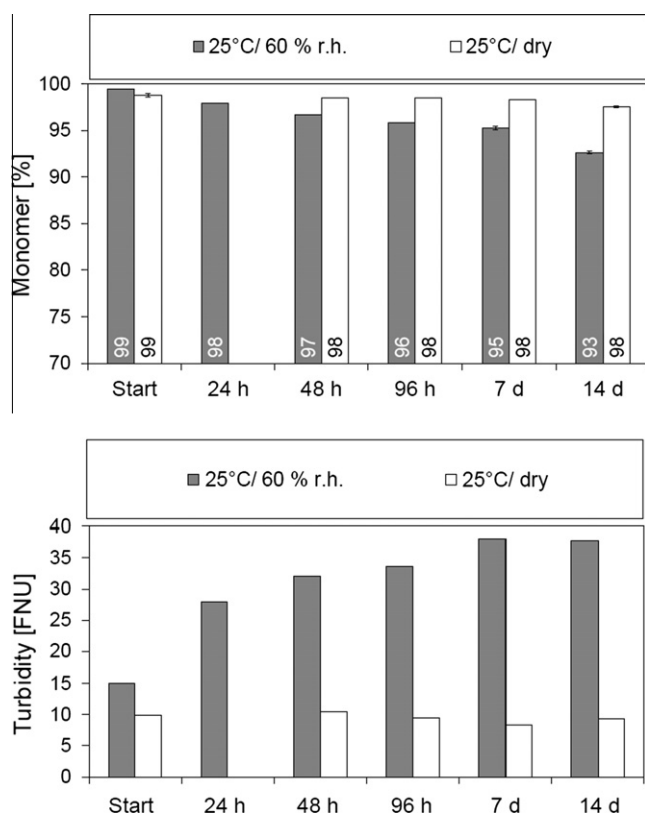


Fig. 10. Storage stability studies of dried mAb I PCMC powder – monomer content and turbidity data after moist or dry storage at 25 °C in glass vials.

potential transformation as regards protein integrity. PCMC of mAb I was dried using dry air and stored at various conditions in glass vials for 6 months. A microscopic image of mAb I glycine PCMC (not shown) in methyl propanol directly after manufacture reveals crystals of cubic and needle like form. After storage at 60% relative humidity at room temperature, rapidly within hours, the α - and then the γ -glycine modification form as opposed to storage under dry conditions (at 4 °C or 25 °C) which preserves the β -glycine form (Fig. 9b). At elevated temperatures (40 °C), a conversion into the α -form occurs after 1 month in a slower process (Fig. 9a).

Along with the polymorphic transformation under moist condition, protein integrity decreases very fast even after 24 h as as-

sessed again by HPSEC and turbidity measurements. Upon dry storage, no such changes were observed (Fig. 10). At 4 °C and dry conditions even after 6 months storage, the monomer content remained unchanged at 98% as did the turbidity value (data not shown). As a consequence, it is recommended to store PCMC products protected from moisture as it is typically recommended for lyophilised formulations.

4. Conclusions

Various models of impingement jet mixers for the production of protein-coated microcrystals (PCMC) were compared. In order to ascertain the greatest impact of the process conditions and type of mixing equipment, a very sensitive model protein, trypsin, and a suboptimal formulation were chosen. All the mixers produced fast and homogeneous mixtures, despite the technically challenging volume ratio of the protein-carrier solution and the anti-solvent solution of 5:95. Microimpingement mixers (bore size <1 μ m) were not suitable for long continuous precipitations due to rapid blockage. By increasing the bore size of the mixers to 2–3.2 mm, the resulting particle size of the PCMC increased and protein recovery on the crystalline carrier surface decreased rapidly. However, particle size and protein recovery along with mixing, diffusion and precipitation performance inside the impingement jet mixers significantly improved with higher flow rates. Indirect ultrasound assisted precipitation at low flow rates is a second option. In all experiments with ultrasound, no blockage of the mixer or the outlet tube by precipitates was observed, which clearly constitutes a big advantage.

At a laminar flow rate, two or four anti-solvent jets (sandwich effect) led to improved mixing of the two liquids. This mixing improvement in the order $SJI < DJI < QJI$ was demonstrated by computational fluid dynamic simulations and the Villermaux–Dushman reaction. The precipitation reactions did not quite follow this ranking, but revealed that the most robust performance as regards time to turbidity ≥ 120 FNU and particle size over a range of flow rates can be achieved by using the QJI.

50–80 L of PCMC suspensions were continuously produced with a QJI mixer made of stainless steel with a bore size of 3 mm. 18 bar was the maximum pressure peak observed, which was still processable by the gear pumps used. The goal to demonstrate manufacture of a pilot-scale volume of PCMC suspension (corresponding to 500 g precipitate) within one shift was readily achieved. If carriers which crystallize in various polymorphic forms are used, dry storage seems to be recommended to avoid a change in modification along with a decrease in monomer. At protein loading rates of 10% or less, the carrier is predominantly crystalline.

Acknowledgement

This work was supported by Boehringer Ingelheim Pharma GmbH and Co. KG.

References

- [1] M.C. Manning, K. Patel, R.T. Borchardt, Stability of protein pharmaceuticals, *Pharmaceutical Research* 6 (11) (1989) 903–918.
- [2] K. Schumacher, G. Winter, M.H.C. Mahler, Instabilitäten von Proteinarzneimitteln, *PZ Prisma* 10 (1) (2003) 15–18.
- [3] W. Wang, S. Singh, D.L. Zeng, K. King, S. Nema, Antibody structure, instability, and formulation, *Journal of Pharmaceutical Sciences* 96 (1) (2007) 1–26.
- [4] J.F. Carpenter, B.S. Chang, W. Garzon-Rodriguez, T.W. Randolph, Rational design of stable lyophilized protein formulations: theory and practice, *Pharmaceutical Biotechnology* 13 (2002) 109–133.
- [5] M.C. Lai, E.M. Topp, Solid-state chemical stability of proteins and peptides, *Journal of Pharmaceutical Sciences* 88 (5) (1999) 489–500.
- [6] S. Schuele, Stabilization of Antibodies in spray dried Powders for Inhalation, LMU University Munich, Dissertation, 2005.

- [7] V. Kumar, V.K. Sharma, D.S. Kalonia, In situ precipitation and vacuum drying of interferon alpha-2a: development of a single-step process for obtaining dry, stable protein formulation, *International Journal of Pharmaceutics* 366 (1–2) (2009) 88–98.
- [8] H. Gieseler, Product Morphology and Drying Behavior Delineated by a New Freeze-drying Microbalance. Naturwissenschaftliche Fakultät der Friedrich-Alexander-Universität Erlangen-Nürnberg, 2004.
- [9] Maa YF, Nguyen PA, inventors; Genentech I, assignee. Method of spray freeze drying proteins for pharmaceutical administration. US patent 6284282. 1999 Apr 27.
- [10] N. Jovanovic, A. Bouchard, G.W. Hofland, G.J. Witkamp, D.J.A. Crommelin, W. Jiskoot, Stabilization of proteins in dry powder formulations using supercritical fluid technology, *Pharmaceutical Research* 21 (11) (2004) 1955–1969.
- [11] E. Reverchon, Supercritical antisolvent precipitation of micro- and nanoparticles, *The Journal of Supercritical Fluids* 15 (1) (1999) 1–21.
- [12] S.P. Cape, J.A. Villa, E.T.S. Huang, T.H. Yang, J.F. Carpenter, R.E. Sievers, Preparation of active proteins, vaccines and pharmaceuticals as fine powders using supercritical or near-critical fluids, *Pharmaceutical Research* 25 (9) (2008) 1967–1990.
- [13] B. Shenoy, Y. Wang, W. Shan, A.L. Margolin, Stability of crystalline proteins, *Biotechnology and Bioengineering* 73 (5) (2001) 358–369.
- [14] K.A. Johnson, Preparation of peptide and protein powders for inhalation, *Advanced Drug Delivery Reviews* 26 (1) (1997) 3–15.
- [15] B.D. Moore, M. Parker, P.J. Halling, J. Partridge, H.N.E. Stevens, Inventors; WO 00/69887 Rapid Dehydration of Proteins, 2000.
- [16] J. Partridge, P.R. Dennison, B.D. Moore, P.J. Halling, Activity and mobility of subtilisin in low water organic media: hydration is more important than solvent dielectric, *Biochimica et Biophysica Acta (BBA)/Protein Structure and Molecular Enzymology* 1386 (1) (1998) 79–89.
- [17] S. Murdan, S. Somavarapu, A.C. Ross, H.O. Alpar, M.C. Parker, Immobilisation of vaccines onto micro-crystals for enhanced thermal stability, *International Journal of Pharmaceutics* 296 (1–2) (2005) 117–121.
- [18] A. Ganesan, N.C. Price, S.M. Kelly, I. Petry, B.D. Moore, P.J. Halling, Circular dichroism studies of subtilisin Carlsberg immobilised on micron sized silica particles, *BBA-Proteins and Proteomics* 1764 (6) (2006) 1119–1125.
- [19] M. Kreiner, J.F.A. Fernandes, N. O'Farrell, P.J. Halling, M.C. Parker, Stability of protein-coated microcrystals in organic solvents, *Journal of Molecular Catalysis B: Enzymatic* 33 (3–6) (2005) 65–72.
- [20] B.K. Johnson, R.K. Prud'Homme, Chemical processing and micromixing in confined impinging jets, *AIChE Journal* 49 (9) (2003) 2264–2282.
- [21] J.L. Luche, *Synthetic Organic Sonochemistry*, Plenum Press, New York, 1998.
- [22] I.L.M. Verschuren, Feed Stream Mixing in Stirred Tank Reactors, Ph.D. Thesis. Technische Universiteit Eindhoven, 2001. ISBN 90-386-2942-7.